Photoinduced Disproportionation of Ru(bpy)$_3$$^{2+}$ on Porous Vycor Glass

Theresa Kennelly,[†] Harry D. Gafney,*[†] and Martin Braun[‡]

Contribution from the Departments of Chemistry and Mathematics, City University of New York, Queens College, Flushing, New York 11367. Received October 2, 1984

Abstract: Tris(2,2′-bipyridine)ruthenium(II), Ru(bpy)$_3$$^{2+}$, cation exchanges onto porous Vycor glass, and the adsorbed complex retains spectral properties equivalent to those in fluid solution. Photolysis (450 nm) of the adsorbate leads to disproportionation, and optical and ESR spectra show that both redox products are stable. The emission polarization ratio, 0.12 ± 0.03 at room temperature, indicates that the reaction occurs between a fixed array of adsorbate ions. Biphotonic excitation of an individual adsorbate ion causes ionization, and the photodetached electron is detected as a transient minimum in the emission decay. Analysis indicates that this emission minimum cannot be attributed to solely an inner filter effect. A model, which reproduces these decays, suggests that the photodetached electron initially populates surface sites, and thermal excitation of the site, arising from nonradiative decay, initiates subsequent reactions since a 3–4-μs delay proceeds [Ru(bpy)$_2$(bpy$^-$)]$^+$ appearance. The reaction efficiency is limited by the photoionization yield, 0.0012, and competition between product formation and recombination, the latter being the dominant process. A narrow dependence of quantum yield on moles adsorbed suggests that disproportionation occurs when the mean separation between the adsorbate ions is within the electron migration distance, 50 ± 10 Å, and when this distance exceeds that for the thermal back reaction, ≤13 Å, the redox products are stable.

Excitation of the 452-nm charge-transfer adsorption of tris-(2,2′-bipyridine)ruthenium(II), Ru(bpy)$_3$$^{2+}$, leads to efficient population of an emissive MLCT state which exhibits a facile redox chemistry.[1-14] The oxidation and reduction potentials of the luminescent MLCT state, 0.84 and 0.77 V (vs. NHE),[3,5,7] respectively, represent a conversion of light energy into redox potential. However, photoinduced electron transfer gives rise to a thermally inverted system, which spawns a rapid, exergonic back reaction. Consequently, the conversion is transitory and, in spite of significant advances in understanding the photoinduced electron-transfer step, preventing the accompanying back reaction, in the absence of a sacrificial reagent, remains a significant experimental challenge.

Recent effort has focused on heterogeneous media or various supports to impose some constraint on the reaction system.[15-24] Gratzel and others have established that dispersions of the n-type semiconductor TiO$_2$ significantly reduce reversibility.[25-29] Photolysis of Ru(bpy)$_3$$^{2+}$ adsorbed onto micron-diameter particles of TiO$_2$ induces a charge separation which not only allows electron migration to a catalyzed reaction site, but an accumulation of electron density sufficient for subsequent multielectron reaction. These systems have been termed "photochemical diodes"[30] since the apparent mechanism is electron transfer into the conduction band.[25,26,31] Although band bending promotes charge separation, Kajiwara and co-workers suggest that recombination of the injected electron and the oxidized complex accounts, in part, for the relatively low yield of H$_2$.[32]

In addition to metal oxide surfaces, there is a growing body of evidence that other supports, particularly hydroxylated silicas and cellulose films (where charge transfer via population of a bulk conduction band is energetically unlikely), also promote charge separation. Calvin and Willner and their co-workers, for example, have shown that the high surface potential of colloidal SiO$_2$, −170 mV, and/or hydrophobic–hydrophilic interactions at the interface reduce the rate of the back reaction.[33-36] In the presence of an electron donor, repulsion between the anionic reduction product and the colloid surface allows an accumulation of electron-transfer products. In addition to interfacial phenomena, experiments with cationic reagents allude to other mechanisms of charge separation. Wheeler and Thomas report that incorporating Ru(bpy)$_3$$^{2+}$ into a silica colloid just below the SiO$_2$–H$_2$O surface enhances the yield of electron transfer between the incorporated complex and methylviologen, MV^{2+}.[37] The anionic nature of the colloid surface and the solubility of these reagents in water suggest, in our opinion,

that both reagents are adsorbed at the time of electron transfer. Yet, in the presence of triethanolamine, the yield of MV$^+$ is within

(1) Gafney, H. D.; Adamson, A. W. *J. Am. Chem. Soc.* **1972**, *94*, 8238.
(2) Bock, C. R.; Meyer, T. J.; Whitten, D. G. *J. Am. Chem. Soc.* **1974**, *96*, 4710.
(3) Navon, G.; Sutin, N., *Inorg. Chem.* **1974**, *13*, 2159.
(4) Lawrence, G. S.; Balzani, V., *Inorg. Chem.* **1974**, *13*, 2976.
(5) Bock, C. R.; Meyer, T. J.; Whitten, D. G., *J. Am. Chem. Soc.* **1975**, *97*, 2909.
(6) Young, R. C.; Meyer, T. J.; Whitten, D. G. *J. Am. Chem. Soc.* **1975**, *97*, 4781.
(7) Creutz, C.; Sutin, N. *J. Am. Chem. Soc.* **1976**, *98*, 6384.
(8) Toma, H. E.; Creutz, C., *Inorg. Chem.* **1977**, *16*, 545.
(9) Lin, C. T.; Bottcher, W.; Chou, M.; Creutz, C.; Sutin, N. *J. Am. Chem. Soc.* **1976**, *98*, 6536.
(10) Young, R. C.; Keene, F. R.; Meyer, T. J. *J. Am. Chem. Soc.* **1977**, *99*, 2468.
(11) Wight, C. A.; Turley, T. J.; Demas, J. N. *J. Chem. Phys.* **1978**, *68*, 5486.
(12) Krist, K.; Gafney, H. D. *J. Phys. Chem.* **1982**, *86*, 951.
(13) Meyer, T. J. *Acc. Chem. Res.* **1978**, *11*, 94.
(14) Kalyanasundram, K. *Coord. Chem. Rev.* **1982**, *46*, 159.
(15) Porter, G. *Pure Appl. Chem.* **1978**, *50*, 263.
(16) Kalyanasundram, K. *Chem. Soc. Rev.* **1978**, *7*, 453.
(17) Turro, N. J.; Gratzel, M.; Braun, A. M. *Angew. Chem., Int. Ed. Engl.* **1980**, *19*, 675.
(18) Gratzel, M. *Isr. J. Chem.* **1979**, *18*, 264.
(19) Thomas, J. K. *Chem. Rev.* **1980**, *80*, 283.
(20) Matsuo, T.; Takuma, K.; Nishizima, T.; Tsutsui, Y. *J. Coord. Chem.* **1980**, *10*, 195.
(21) Rodgers, M. A. J.; Becker, J. C. *J. Phys. Chem.* **1980**, *84*, 2762.
(22) Atik, S. S.; Thomas, J. K. *J. Am. Chem. Soc.* **1981**, *103*, 7403.
(23) Ford, W. E.; Otvos, J. W.; Calvin, M. *Nature (London)* **1978**, *274*, 507.
(24) Nomura, T.; Escabi-Perez, J. R.; Sunamoto, J.; Fendler, J. H. *J. Am. Chem. Soc.* **1980**, *102*, 1484.
(25) Gratzel, M. *Acc. Chem. Res.* **1981**, *14*, 376.
(26) Borgarello, E.; Kiwi, J.; Pelizzetti, E.; Visca, M.; Gratzel, M. *Nature (London)* **1981**, *283*, 158.
(27) Kawai, T.; Sakata, T. *Nouv. J. Chim.* **1981**, *5*, 279.
(28) Sato, S.; White, J. M. *J. Phys. Chem.* **1981**, *85*, 592.
(29) Lehn, J. M.; Sauvage, J. P.; Ziessel, R. *Nouv. J. Chim.* **1980**, *4*, 623.
(30) Novak, A. J. *Appl. Phys. Lett.* **1977**, *30*, 567.
(31) Clark, W. D.; Sutin, N. *J. Am. Chem. Soc.* **1977**, *99*, 4676.
(32) Kajiwara, T.; Hasimoto, K.; Kawal, T.; Sakata, T. *J. Phys. Chem.* **1982**, *86*, 4516.
(33) Willner, I.; Otvos, J. W.; Calvin, M. *J. Am. Chem. Soc.* **1981**, *103*, 3203.

[†] Department of Chemistry.
[‡] Department of Mathematics.

experimental error of that in aqueous solution.[37] These investigators propose that the SiO_2 particle enhances charge separation by electron tunneling between $Ru(bpy)_3^{2+}$ trapped in the particle and MV^{2+} on the surface; the latter then escapes into the bulk solvent.

Recently, Milosavijevic and Thomas reported that photolysis of $Ru(bpy)_3^{2+}$ adsorbed onto "dry" cellulose films leads to disproportionation.[38] The reaction involves triplet–triplet annihilation, which appears to occur over distances larger than the sum of the molecular diameters, followed by electron transfer. The stability of $[Ru(bpy)_2(bpy^-)]^+$, some of which persists indefinitely, is attributed to reduction of $Ru(bpy)_3^{3+}$ by the cellulose support, the latter being competitive with the thermal back reaction. As these investigators note, however, the result could mean that small amounts of $Ru(bpy)_3^{3+}$ and $[Ru(bpy)_2(bpy^-)]^+$ can coexist in cellulose. Correlations between driving force and rate are tenuous, but the result is striking since the driving force for the back reaction, ca. 2.5 eV, is the largest that will be encountered in a $Ru(bpy)_3^{2+}$ photoinduced electron-transfer reaction.

Our interest in hydroxylated silicas and disproportionation arises from the observation that 450-nm photolysis of $Ru(bpy)_3^{2+}$ cation exchanged onto porous Vycor glass (PVG) causes disproportionation, and that the optically detectable reduction product, $[Ru(bpy)_2(bpy^-)]^+$, is indefinitely stable.[39] Subsequent ESR experiments indicated that both photoproducts are stable in spite of the ca. 2.5-eV driving force for the back reaction. To understand how this reaction occurs and specifically the means by which PVG, a transparent, hydroxylated silica support, curtails reversibility, the reaction has been examined by steady-state and flash photolysis techniques.

The data indicate a reaction sequence similar to that for disproportionation in aqueous solution.[40] Biphotonic excitation of an individual adsorbate ion induces ionization, the photodetached electron appearing as a minimum in the emission decay. However, emission polarization measurements indicate that the reaction occurs between a fixed array of adsorbed reactants. A model, which reproduces the transient decays, as well as a narrow dependence of yield on the moles adsorbed/gram, indicates that two criteria distinguish this surface reaction from that in aqueous solution. First is the availability of surface sites that function as electron acceptors, but following thermal activation, the latter, arising from nonradiative decay, eject an electron to undergo subsequent reactions. Second, the distance between the adsorbed ions is critical. When this distance is within the electron migration distance, 50 ± 10 Å, disproportionation occurs, and if the electron migration distance exceeds that for the thermal back reaction, ≤13 Å, the disproportionation products are stable.

Experimental Section

Materials. $[Ru(bpy)_3]Cl_2$ was prepared according to the procedures of Palmer and Piper and twice recrystallized from distilled water as the chloride salt.[41] Absorption, emission, and resonance Raman spectra of the complex were in excellent agreement with published spectra.[42,43] Gaseous reagents (Linde) were used without further purification since each had a purity of ≥99%. All organic solvents used in these experiments were spectral grade, and aqueous solutions were prepared with water distilled in a Corning distillation unit.

Code 7930 porous Vycor glass containing 70 ± 21 Å diameter cavities was obtained from the Corning Glass Co. Pieces (25 mm × 25 mm × 4 mm) of PVG were continuously extracted, first with acetone for 12 h, and then with distilled water for the same period of time. The extracted pieces were dried under reduced pressure in a vacuum oven at 30 °C and then calcined at 650 °C either in a muffle furnace or under flowing O_2

or H_2 in a tube oven for ≥72 h. The calcined PVG samples were transferred while hot to a vacuum desiccator and cooled to room temperature under reduced pressure ($p \leq 10^{-4}$ torr).

Impregnation with $Ru(bpy)_3^{2+}$ was by previously described procedures[44] and controlled by varying the concentration of the impregnating solution and/or the exposure time. Generally, 50 mL of aqueous solution, ranging from 10^{-6} to 10^{-3} M in $[Ru(bpy)_3]Cl_2$, was added and the samples were soaked for 4 to 12 h. UV–visible spectra of the solution phase were recorded periodically and the moles of complex adsorbed were calculated from the change in optical density. Unless otherwise specified all experiments were performed on "dry" samples; ≥99.97% by weight of the water incorporated during impregnation was removed under vacuum, $p \leq 10^{-4}$ torr, at room temperature, or in a vacuum oven at 40 °C. Although the term dry is used to specify removal of the bulk water, diffuse reflectance FTIR spectra of the impregnated samples indicated that a considerable amount of chemisorbed water remained. The impregnated PVG samples used in these experiments contain from 3.15 × 10^{-7} to 5.49 × 10^{-4} mol or 7.01 × 10^{-8} to 1.22 × 10^{-4} mol of Ru-$(bpy)_3^{2+}(ads)/g$ of PVG.

Photolysis Procedures. Since PVG is transparent at the excitation and analyzing wavelengths used in these experiments, the experimental procedures are similar to those used with fluid solutions. The impregnated PVG samples were rigidly mounted with a Teflon holder in previously described 4 cm × 2.2 cm × 1 cm rectangular quartz or Pyrex cells.[44,45] The cell and enclosed sampled were evacuated ($p \leq 10^{-4}$ torr) and irradiated with a 350-W Illumination Industries Xe arc lamp. The lamp output was collimated and passed through a 12-cm quartz cell filled with distilled water to remove IR radiation and then through a Plexiglass filter (50% transmission at 351 nm) which limited the excitation to the 452-nm MLCT transition of the adsorbed complex. A Spectra Physics Model 164-08 Ar laser was used for monochromatic irradiations at 457.9, 488.0, or 514.5 nm. The laser intensity incident on the front surface of the photolysis cell was measured with a Coherent Model 210 power meter, and the intensity absorbed by $Ru(bpy)_3^{2+}(ads)$, I_a, was calculated from an average of the initial and final absorbance of the complex at the excitation wavelength. The moles of reactant consumed and product formed were calculated according to the procedure of Wong and Allen assuming that the ratio of reactant and product effective extinction coefficients (k in ref 46) is equivalent to that in aqueous solution.[46] The assumption is justified by the similarity of the spectra in the two media (see Results).

Because of limited diffusion on the PVG surface, photolysis generates an inhomogeneous sample, and the persistent experimental difficulty was to assure that the region analyzed corresponded to the region irradiated. To ensure this correspondence, the cell was mounted in a holder and irradiated through a 6.5-mm diameter hole at its center. The entire unit was then placed in the spectrophotometer where pins in the sample compartment aligned it with the spectrophotometer light beam. To quantitate the photochemical reaction parameters, however, the samples were photolyzed and analyzed simultaneously.

The cell containing the impregnated sample was placed in a holder which defined four 6.5-mm diameter regions near each corner of the PVG sample. The holder was attached to a bidirectional translational mount which allowed four separate photolyses of the same sample. The photolyzing laser beam, expanded with a lense to completely irradiate one defined sample region, impinged onto the sample at an angle of 6° from the normal to the PVG surface. The excitation intensity was varied from 6.5 × 10^{-8} to 7.8 × 10^{-7} einsteins/s-cm^2 by the laser current and/or neutral density filters (Klinger Scientific). The photochemical change was monitored with a collimated beam, perpendicular to the PVG surface, from a 100-W Xe lamp powered by a Sola filtered dc power supply. A filter (Klinger Scientific) prior to the sample limited the analyzing light to ≥475 nm. After passing through the sample, the analyzing light was focused onto the entrance slit of a Bausch and Lomb Model 33-86-08 grating monochromator. The photolysis-analysis geometry probed 96% of the exposed volume, and minimized the amount of scattered laser light entering the monochromator. The change in intensity of the analyzing light was monitored with a Hamamatsu R928 photomultiplier powered by a Pacific Photometric Instruments Model 203 power supply. The PM current was dropped across a 1 kΩ resistor, and the time dependence of the voltage change was recorded on a Varian Model A-25 recorder.

The cell holder and photolysis-analysis geometry described above were also used in the flash photolysis experiments. The impregnated sample was excited with a 450 ± 20 nm pulse (fwhm 150 ns) from a 10^{-5} M ethanol solution of Coumarin 450 (Exiton Chemical Co.) pumped by a

(34) Willner, I.; Yang, J. M.; Laane, C.; Otvos, J. W.; Calvin, M. *J. Phys. Chem.* **1981**, *85*, 3277.
(35) Willner, I.; Degani, Y. *Chem. Commun.* **1982**, 761.
(36) Willner, I.; Degani, Y. *J. Am. Chem. Soc.* **1983**, *105*, 6228.
(37) Wheeler, J.; Thomas, J. K. *J. Phys. Chem.* **1982**, *86*, 4540.
(38) Milosavijevic, B. H.; Thomas, J. K. *J. Phys. Chem.* **1983**, *87*, 616.
(39) Kennelly, T.; Gafney, H. D. *J. Inorg. Nucl. Chem.* **1981**, *43*, 2988.
(40) Meisel, D.; Matheson, M. S.; Mulac, W. A.; Rabini, J. *J. Phys. Chem.* **1977**, *81*, 1449.
(41) Palmer, R. A.; Piper, T. S. *Inorg. Chem.* **1966**, *5*, 864.
(42) Demas, J. N.; Crosby, G. A. *J. Am. Chem. Soc.* **1971**, *93*, 2841.
(43) Braunstein, C. H.; Baker, A. D.; Strekas, T. C.; Gafney, H. D. *Inorg. Chem.* **1984**, *23*, 857.

(44) Wolfgang, S.; Gafney, H. D. *J. Phys. Chem.* **1983**, *87*, 5395.
(45) Basu, A.; Gafney, H. D.; Perettie, D. J.; Clark, J. B. *J. Phys. Chem.* **1983**, *87*, 4532.
(46) Wong, P. K.; Allen, A. D. *J. Phys. Chem.* **1970**, *74*, 774.

Photoinduced Disproportionation of Ru(bpy)₃²⁺

J. Am. Chem. Soc., Vol. 107, No. 15, 1985 4433

Candella Corp. coaxial flash lamp. The laser pulse intensity was varied by changing the voltage applied to the flash lamp capacitor, 12 to 25 kV, by a Walden Model 545A high-voltage power supply. A lense focused the laser pulse onto the PVG sample region defined by a 6.5-mm hole of the cell holder. Following excitation, the change in intensity of the analyzing beam was monitored with the above monochromator–photomultiplier combination. The excitation pulse is extensively scattered by this porous support, and to prevent its reaching the detector, a filter (Klinger Scientific) which transmits at $\geq$490 nm was placed between the sample and the monochromator. The PM current was dropped across a 750-ohm resistor, and the time dependence of the voltage was displayed on a Hewlett-Packard Model 175A oscilloscope and photographed with a Polaroid camera. The RC time constant of the detection circuit was 22 ns, and the scope trace was triggered off the discharge of the capacitor driving the flash lamp. Tests with untreated PVG samples established that the time resolution of the apparatus was limited by the laser pulse duration, 150 ns, when monitored in the 490- to 550-nm region, and slightly shorter, ca. 100 ns, when monitored at longer wavelengths.

Physical Measurements. Possible gaseous photoproducts were collected with a Toepler pump and analyzed by previously described gas chromatographic techniques.[47,48] UV–visible spectra were recorded on a Cary 14 or Techtron 635 spectrophotometer adapted to hold the rectangular cells. Emission spectra were recorded on a Perkin-Elmer Hitachi MPF-2A emission spectrophotometer equipped with a Hamamatsu R818 red-sensitive photomultiplier. The sample arrangement within the emission spectrophotometer has been previously described.[44] Emission decay rates, following low-intensity excitation with an Ortec nanosecond light pulser (fwhm 6–8 ns), were measured by previously described signal-averaging techniques.[44] EPR spectra of the adsorbed photoproducts were recorded at room temperature, 22 $\pm$ 1 °C or 77 K, on an IBM-Bruker Model ER200E-SCR spectrometer. The photoproducts were generated by photolysis in the spectrometer cavity with the filtered 350-W Xe lamp (see above), the spectra recorded during photolysis were independent of whether crushed (60–80 mesh) or solid (4 mm × 4 mm × 12 mm) impregnated PVG samples were used. No EPR resonances were detected when unimpregnated; cleaned PVG samples were irradiated under identical conditions.

The resonance Raman spectrometer has been previously described,[49] and the spectra described in this paper were recorded by means of 90° transverse excitation with the 457.9- or 514.5-nm Ar laser lines. Absorption spectra recorded before and after scanning the resonance Raman spectrum showed no detectable photochemical change. pH measurements were made with a Beckman Expandomatic SS-2 pH meter equipped with a glass combination electrode, and calibrated with standard buffers. This instrument, but equipped with an Orion chloride ion specific electrode calibrated with standard NaCl solutions, was used to monitor the aqueous phase [Cl⁻] during impregnation.

Results

Adsorption Studies. Thermal gravimetric analysis of PVG shows that water desorbs in three distinct steps. A rapid decline of ca. 1% in sample weight at 100–120 °C marks the loss of bulk water from the 70 $\pm$ 21 Å cavities. A slower weight loss from 120 to ca. 700 °C indicates desorption of chemisorbed water, the latter being hydrogen bonded in varying degrees to the silanol groups. At ca. 700 °C, a large, rapid weight loss marks the onset of condensation to a nonporous glass.

Dispersed in distilled water, 100 μg/mL, pulverized PVG develops a ζ potential of -26 ± 2 mV.[45] The anionic potential relative to the bulk solvent induces, as shown in Figure 1, adsorption of the cationic complex with no detectable adsorption of the anionic counterion. After 24 h, for example, 64% of the Ru(bpy)₃²⁺, but $\leq$2% of the Cl⁻, is adsorbed when a 1.248-g piece of PVG is placed in a 1.03 × 10⁻⁴ M [Ru(bpy)₃]Cl₂ solution. Like other hydrated silicas with slightly acidic (p$K_a \sim$ 9) silanol groups, PVG is a cation exchanger,[50] and diffuse reflectance FTIR indicate that complex is bound to a surface consisting of free silanol groups, 3750 cm⁻¹, and chemisorbed water, 3500 cm⁻¹.[51-53]

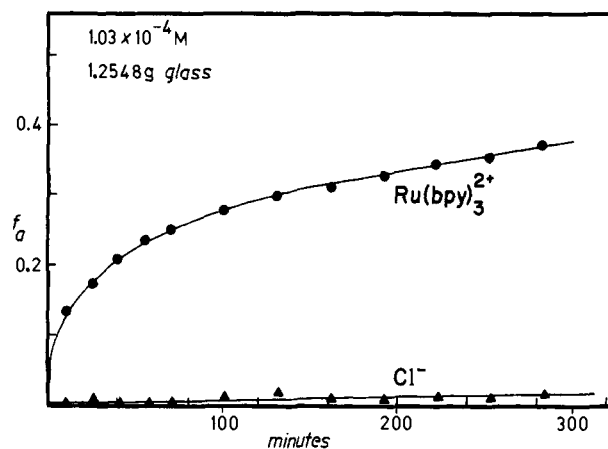**Figure 1.** The fraction of Ru(bpy)₃²⁺ and Cl⁻ adsorbed onto a 1.2548-g sample of PVG from a 1.03 × 10⁻⁴ M Ru(bpy)₃Cl₂ solution.

Generally, three PVG samples are impregnated simultaneously. After removal of the water incorporated during impregnation, adsorption spectra of the individual samples and spectra recorded at different locations on the same sample are within experimental error.[54] The agreement establishes reproducible impregnation and a uniform distribution of Ru(bpy)₃²⁺(ads) on the PVG surface. However, previously described grinding and optical density measurements indicate a nonuniform cross-sectional distribution.[44] Regardless of the moles adsorbed, Ru(bpy)₃²⁺ penetrates 0.4 $\pm$ 0.1 mm into PVG, and leads to impregnation of regions adjacent to the outer geometric surfaces of the samples. Penetration depth is a kinetic parameter controlled principally by exposure times longer than the 4 to 12 h used in these experiments.[55] Within the impregnated regions, the optical density due to Ru(bpy)₃²⁺(ads) declines linearly with thickness, i.e., optical path length, which implies that the moles of Ru(bpy)₃²⁺(ads)/unit volume of PVG is constant.

Spectroscopic Properties of Ru(bpy)₃²⁺(ads). In the 260- to 500-nm region, the UV–visible absorption spectrum of Ru(bpy)₃²⁺(ads) is within experimental error in band maxima, relative extinction coefficient, and band half-width of the spectrum of the complex in aqueous solution.[56] The absolute extinction coefficients of Ru(bpy)₃²⁺(ads), calculated assuming an optical path length equivalent to the penetration depth, are 10 to 15% larger than those in aqueous solution. The actual difference is most likely smaller since light scattering by the PVG samples introduces an inherent spectroscopic uncertainty of $\sim$8%[54] from sample to sample, and there is a 20% uncertainty in penetration depth.[44] The latter describes cross-sectional distribution in the general sense, but it is not an accurate measure of the optical path length.

Resonance Raman spectra of the adsorbed complex and that in aqueous solution differ by $\leq$1 cm⁻¹ in the seven bipyridine vibrational frequencies.[56] The relative band intensities are also equivalent in both media with the exception of the 1492-cm⁻¹ vibration of the adsorbed complex. The intensity of this band relative to that of the 1609-cm⁻¹ vibration is 4.4 for the complex in aqueous solution, but only 2.5 for the adsorbed complex. The similarity of the frequencies and the absence of detectable splitting of the bands establishes that the ground state of the adsorbed complex is equivalent to that in aqueous solution. The change in intensity, however, implies that the structure of the excited state of the adsorbed complex differs from that in aqueous solution.[57]

The emission maximum occurs at 610 nm, and the emission intensity increases linearly with the fraction of light adsorbed by Ru(bpy)₃²⁺ads. However, at the highest loadings, ca. 2 × 10⁻⁴

(47) Simon, R.; Morse, D. L.; Gafney, H. D. *Inorg. Chem.* **1983**, *22*, 573.
(48) Simon, R. Ph.D. Thesis, City University of New York, 1983.
(49) Basu, A.; Gafney, H. D.; Strekas, T. C. *Inorg. Chem.* **1982**, *21*, 2231.
(50) Burwell, R. L., CHEMTECH **1970**, 370.
(51) Sidorov, A. N. *Opt. Spectrosc. (USSR)* **1960**, *8*, 424.
(52) Cant, N. W.; Little, L. H. *Can. J. Chem.* **1964**, *42*, 802.
(53) Elmer, T. H.; Chapman, I. D.; Nordberg, M. E. *J. Phys. Chem.* **1962**, *66*, 1517.

(54) The experimental error in a spectral comparison of PVG samples is $\leq$8%. This arises principally from differences in light scattering by the random internal pore structure.
(55) Wolfgang, S. PhD. Thesis, City University of New York, 1983.
(56) Shi, W.; Wolfgang, S.; Strekas, T. C.; Gafney, H. D., *J. Phys. Chem.* **1985**, *89*, 0000.
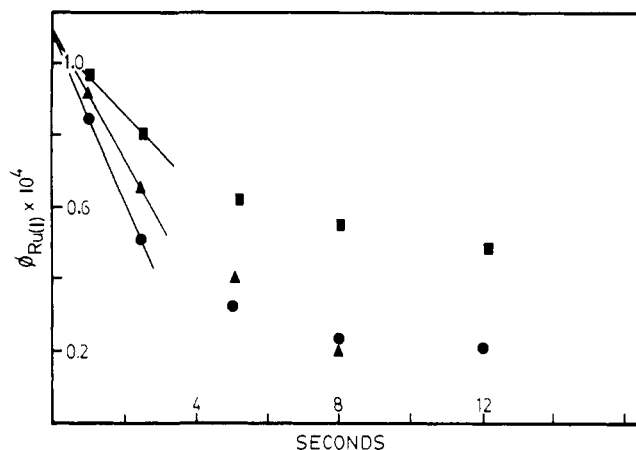(57) Washel, A. *Annu. Rev. Biophys. Bioeng.* **1977**, *6*, 273.

Figure 2. The change in ϕ_{Ru1} during irradiation of a sample containing 2.06×10^{-6} mol of $Ru(bpy)_3{}^{2+}(ads)/g$ with 457.9- (●), 488.0- (▲), and 514.5-nm (■) light.

mol/g, the intensity is reduced by 20% relative to a deaerated aqueous solution of equivalent optical density at the 450-nm excitation wavelength.[56] At lower loadings where self-quenching does not occur, the emission quantum yield, ϕ_{em}, of the adsorbed complex is 0.12 ± 0.03,[56] and, following low intensity excitation, the emission intensity decays exponentially with a lifetime ($1/e$) of 740 ± 20 ns.[58]

Steady-State Photolyses. Difference spectra recorded during 457.9-nm photolysis of $Ru(bpy)_3{}^{2+}(ads)$ in vacuo show a decline in absorbance at 452 nm, characteristic of the adsorbed complex, and concurrent increases at 350 and 510 nm.[39] The spectral changes are independent of whether PVG is calcined in an oxidizing, O_2, or reducing, H_2, atmosphere prior to impregnation, and GC analyses of the cell contents following photolysis give no indication of O_2, H_2, or hydrocarbon photoproducts. The spectral changes are equivalent to those observed during pulse radiolytic reduction of $Ru(bpy)_3{}^{2+}$ [59-61] or reductive quenching of its MLCT state by Eu^{2+},[7] and establish formation of $[Ru(bpy)_2(bpy^-)]^+(ads)$ (bpy$^-$ denotes the radical anion). In vacuo, the spectrum of $[Ru(bpy)_2(bpy^-)]^+(ads)$ persists for ≥ 48 h,[39] but could be reversed by exposure to 1 atm of O_2 where the spectral changes correspond to recovery of 90 to 97% of $Ru(bpy)_3{}^{2+}(ads)$.

EPR spectra recorded periodically during photolysis of samples in vacuo also confirm formation of the reduced complex and indicate the presence of another paramagnetic photoproduct. Concurrent with the increase in absorbance at 510 nm, a slightly asymmetric signal developes with $g = 2.0086$ and a peak-to-peak line width of 25 ± 2 G at 22 ± 1 °C.[39] DeArmond and Carlin report that electrochemically generated $[Ru(bpy)_2(bpy^-)]^+$ in CH_3CN exhibits a similar asymmetric signal with $g = 1.998$.[62] The peak-to-peak line width of the latter is 90 G at room temperature, but decreases to ca. 26 G at 77 K.[62,63] The asymmetric resonance, attributed to $[Ru(bpy)_2(bpy^-)]^+(ads)$, is superimposed on a broad signal with $g = 2.09$ and a peak-to-peak line width of 350 ± 15 G. The intensities of both resonances increase with irradiation time and the resonances remain unchanged for at least 2 h after photolysis. Since EPR spectra of frozen, 77 K, solutions of $Ru(bpy)_3{}^{3+}$, generated by Cl_2 oxidation of 0.1 N H_2SO_4 solutions of $Ru(bpy)_3{}^{2+}$, show a similar resonance with $g = 2.10$ and a peak-to-peak line width of 360 ± 10 G, the broad resonance is attributed to formation of $Ru(bpy)_3{}^{3+}(ads)$,[64] although the latter
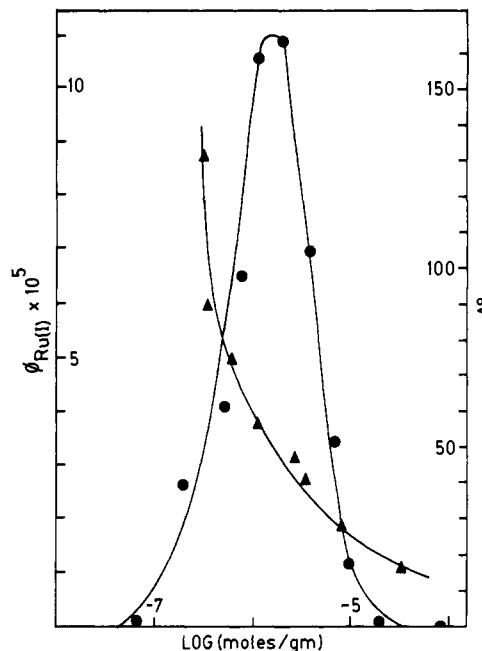
(58) Shi, W.; Gafney, H. D.; Clark, H. D.; Perettie, D. J. *Chem. Phys. Lett.* **1983**, *99*, 253.

(59) Baxendale, J. H.; Fiti, M. *J. Chem. Soc., Dalton Trans.* **1972**, 1995.

(60) Mulazzani, Q. G.; Emmi, S.; Fouchi, P. G.; Ventur, M.; Hoffman, M. Z. *J. Am. Chem. Soc.* **1978**, *100*, 1978.

(61) Meisel, D.; Matheson, M. S.; Rabini, J. *J. Am. Chem. Soc.* **1978**, *100*, 117.

(62) DeArmond, M. K.; Carlin, C. M. *Coord. Chem. Rev.* **1981**, *36*, 325.

(63) Motten, A. G.; Hanck, K.; DeArmond, M. K. *Chem. Phys. Lett.* **1981**, *79*, 541.

(64) DeSimone, R. E.; Drago, R. S. *J. Am. Chem. Soc.* **1970**, *92*, 2343.
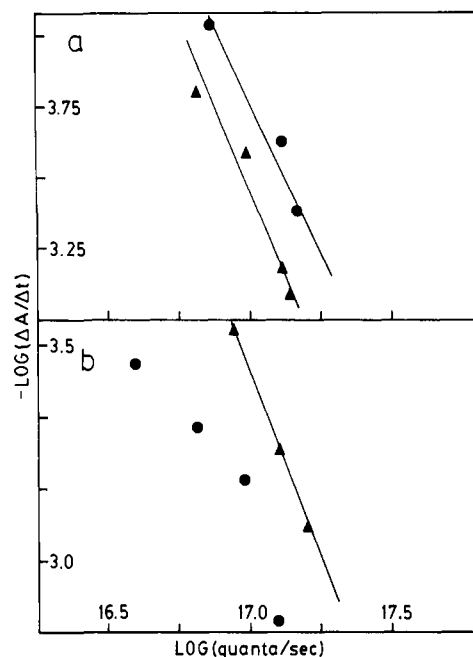

Figure 3. The dependence of ϕ_{Ru1} (●) on the moles of $Ru(bpy)_3{}^{2+}$-(ads)/g, and the calculated mean separation (▲) between the adsorbate ions (see text).

photoproduct is not optically detectable because of its weak absorbance in the visible region, $\epsilon_{675\ nm} = 476$ M^{-1} cm^{-1}.[3] Optically monitoring the rate of formation of $[Ru(bpy)_2(bpy^-)]^+(ads)$ at 510 nm yields 0.48 ± 0.05 as the average moles of $[Ru(bpy)_2-(bpy^-)]^+(ads)$ formed per mole of $Ru(bpy)_3{}^{2+}(ads)$ consumed. The stoichiometry of the reaction is independent of excitation intensity and the initial moles of complex adsorbed (see below).

Since photolysis depletes $Ru(bpy)_3{}^{2+}(ads)$ within the exposed region, and particularly during 514.5-nm photolyses, $[Ru(bpy)_2(bpy^-)]^+(ads)$ formation introduces an inner filter effect; the quantum yields of $[Ru(bpy)_2(bpy^-)]^+(ads)$ formation, ϕ_{Ru1}, are extrapolated from plots, illustrated in Figure 2, of the observed yield vs. irradiation time. The values of ϕ_{Ru1} are independent of excitation at 457.9, 488.0, and 514.5 nm, but exhibit a pronounced dependence on the moles of complex adsorbed/gram of PVG, and the excitation intensity. As illustrated in Figure 3, ϕ_{Ru1} at each excitation wavelength is a surprisingly narrow function of the moles adsorbed. The maximum yield occurs at ca. 2×10^{-6} mol/g and rapidly declines at both higher and lower amounts adsorbed. The declines in efficiency are not due to other competitive photoreactions since difference spectra, EPR spectra, and reaction stoichiometry are independent of the moles of complex/gram of PVG.

Four independent measurements of the intensity dependence are made at different locations on each sample (see Experimental Section). The excitation intensity is varied from 6×10^{-8} to 8×10^{-7} einsteins/s·cm², and the initial rates of formation of $[Ru(bpy)_2(bpy^-)]^+(ads)$ are calculated from recorder traces of the change in absorbance at 500 nm. The first and last measurements on each sample are made at the same intensity and differ by $\leq 15\%$. For those samples which show a detectable photoreaction, plots of log (rate) vs. log (I_a), illustrated in Figure 4, yield slopes of 2.1 ± 0.3. As illustrated, however, plots of some of the more reactive samples, i.e., containing ca. 2×10^{-6} mol/g, are not linear. Although subject to a poor signal-to-noise ratio, the initial rates for these reactive samples are second order in I_a, and there is no spectral evidence indicating either a change in reaction stoichiometry or reaction pathway. Since it is unlikely that the intensity dependence of $[Ru(bpy)_2(bpy^-)]^+(ads)$ formation would change without a change in reaction pathway, the deviation is attributed to the experimental difficulty of measuring the true initial rate, and/or a "saturation effect", in which the intensity dependence approaches first order in these more reactive samples.[38,65]

Photoinduced Disproportionation of Ru(bpy)$_3^{2+}$

J. Am. Chem. Soc., Vol. 107, No. 15, 1985 4435

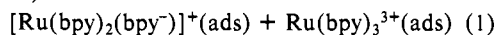**Figure 4.** The dependence of the rate of formation of Ru(bpy)$_2$-(bpy$^-$)$^+$(ads) on the 457.9-nm excitation intensity: (a) 7.76 × 10^{-6} (●) and 5.35 × 10^{-5} mol/g (▲); (b) 2.84 × 10^{-6} (▲) and 2.32 × 10^{-6} mol/g (●).

The reaction products, stoichiometry, and excitation intensity dependence indicate a biphotonic induced disproportionation, i.e.,

$$2Ru(bpy)_3^{2+}(ads) + 2h\nu \rightarrow$$

$$[Ru(bpy)_2(bpy^-)]^+(ads) + Ru(bpy)_3^{3+}(ads) \quad (1)$$

The reaction is equivalent to that following intense flash photolysis of Ru(bpye)$_3^{2+}$ in aqueous solution,[40] but unlike the latter, where the lifetime of [Ru(bpy)$_2$(bpy$^-$)]$^+$ is 2 ± 0.6 ms, [Ru(bpy)$_2$-(bpy$^-$)]$^+$(ads) has a lifetime of 48 h in vacuo.[39] Since EPR spectra of [Ru(bpy)$_2$(bpy$^-$)]$^+$(ads) and particularly Ru(bpy)$_3^{3+}$(ads) do not change for at least 2 h after photolysis, product stability cannot be attributed to a secondary reaction with the support[38] that competitively reduces the oxidized product.

Flash Photolysis Experiments. Excitation of samples containing 2.0 ± 0.3 × 10^{-6} mol of Ru(bpy)$_3^{2+}$(ads)/g of PVG in vacuo with a 150-ns (fwhm), 450 ± 20 nm laser pulse does not induce the immediate formation of [Ru(bpy)$_2$(bpy$^-$)]$^+$(ads). As shown in Figure 5a, monitoring the absorbance at 510 nm, characteristic of the reduced complex, shows no increase either concurrent with the excitation pulse or during the lifetime of the luminescent MLCT state, 740 ± 20 ns. Extending the sweep time to 10 μs, however, indicates that a weak 510-nm absorbance appears 3 to 4 μs after excitation. Multiple exposures of the same region induce a blue coloration, and absorption spectra, recorded after each excitation, show an increase in absorbance at 510 nm. Increasing the excitation intensity, proportional to the square of the laser charging voltage, by varying the latter from 13 to 25 kV, causes more than a 10-fold increase in absorbance, but does not eliminate the delay in product appearance. No set of excitation intensity and/or loading conditions, accessible in these experiments, eliminates the delay in product appearance.

Product appearance is dependent on the oxygen. At 1 atm pressure, O$_2$ quenches the MLCT state of Ru(bpy)$_3^{2+}$(ads),[44] and laser excitation induces a weak emission which decays exponentially, $k = 1.10 ± 05 × 10^6$ s^{-1}, but fails to produce an absorbance at 510 nm. O$_2$ quenching establishes the involvement of the MLCT state, but the delay in product appearance indicates that it is not the immediate precursor to product formation. Rather, one or more reactions intervene between excitation and [Ru-(bpy)$_2$(bpy$^-$)]$^+$(ads) formation.
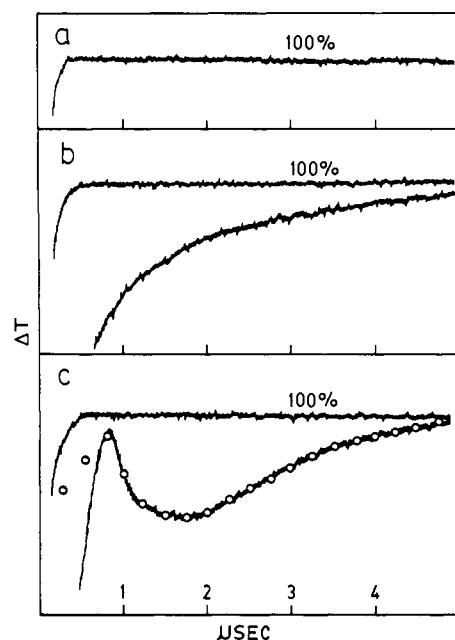
(65) Siram, R.; Endicott, J. F.; Cunningham, K. M. *J. Phys. Chem.* **1981**, *85*, 38.

Figure 5. Traces recorded during flash photolysis of a sample containing 1.91 × 10^{-6} mol of Ru(bpy)$_3^{2+}$(ads)/g: (a) at 510 nm; (b) *Ru-(bpy)$_3^{2+}$(ads) emission decay at 600 nm following low intensity laser excitation. (c) *Ru(bpy)$_3^{2+}$(ads) emission decay at 600 nm following high-intensity laser excitation. Open circles (O) represent calculated emission intensities (see text).

The first detectable photoproduct appears in the 600- to 700-nm region as a distortion of the MLCT emission. Under low-intensity excitation with an Ortec nanosecond light pulser, the emission decays exponentially with a rate constant of 1.35 ± 0.04 × 10^6 s^{-1}.[44] Monitoring the emission at 600 nm following excitation with a low-intensity laser pulse (13.5-kV charging voltage) yields the trace shown in Figure 5b. Although appearing exponential, analysis indicates a complex decay composed of at least two components. A fast component, which decays in ≤150 ns, is followed by a slower component. Plotting the latter according to first-order kinetics yields a rate constant of 3.4 ± 1.0 × 10^5 s^{-1}. Deviations are expected at shorter times because of the preceding fast component, but the unusually small value of the rate constant and deviations at longer times attest to a complex reaction sequence. Indeed, the complexity is evident from the intensity dependence. Increasing the excitation intensity changes not only the signal amplitude, but also its shape. When the excitation intensity is increased by 1.6 (17.2-kV charging voltage), the initial rapid decay is followed by a time span, ca. 0.7 to 1.2-μs, during which the emission intensity is constant. Further increases in excitation intensity cause the emitted intensity to decline in this time region, and the highest excitation intensity accessible in these experiments (25 kV charging voltage) yields the trace shown in Figure 5c. The trace has the appearance of "ringing" in the PM, but it is not an experimental artifact. Repeating the experiment on an unexposed region of the same sample, but under 1 atm of O$_2$, yields an exponential decay with a lifetime of 715 ± 20 ns, which agrees with the decay of the *Ru(bpy)$_3^{2+}$(ads) emission. Pumping out the O$_2$ and repeating the experiment on a third unexposed region of the sample regenerates Figure 5c. Furthermore, excitation of unimpregnated PVG under identical conditions fails to induce any transient absorbance or emission when monitored in the 500- to 800-nm region.

Figures 5b and 5c trace the emission decay at 600 nm following laser excitation. When the flash experiments were repeated in the conventional manner with an analyzing light beam probing the exposed region, however, the minimum in Figure 5c appears as an absorbing transient. Since a decline in emission intensity due only to reactions depopulating the luminescent MLCT state would approach, but not cross the base line, the minimum in Figure 5c must be due to a transient which absorbs the emitted light. Two approaches were used to resolve the absorption spectrum from
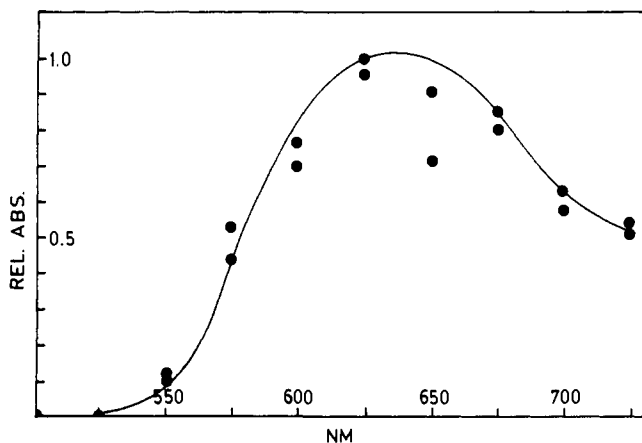
4436 *J. Am. Chem. Soc., Vol. 107, No. 15, 1985*

Kennelly et al.

Figure 6. Relative transient absorbance obtained by exposing samples containing $1.9 \pm 0.1 \times 10^{-6}$ mol/g to a high intensity (22 kV) laser pulse.

the emission. First, the net absorbance was measured with an analyzing beam at 25-nm intervals over the 500- to 725-nm region. Second, without an analyzing beam, the depth of the minimum in the emission was measured relative to an assumed decay similar to that in Figure 5b. Within the spectral limits of the MLCT emission, both yield similar spectra with a 625–650-nm absorption maximum. Figure 6, which illustrates the transient absorption spectrum obtained by the first procedure, resembles that of the solvated electron,[66] and scavenging experiments confirm its presence.

Initially, N_2O was used as a scavenger, but the experiments yield ambiguous results since it quenches the MLCT state.[44] In addition to the mechanistic ambiguity, these experiments raised a more fundamental question regarding the use of a gaseous scavenger. Quenching by a gaseous reagent depends on the amount adsorbed.[44] Most likely, scavenging will also depend on the amount adsorbed which, particularly with a weakly adsorbed species, can vary from sample to sample.[44] Consequently, adsorption of gaseous electron scavengers may not be sufficient to induce a detectable change. For this reason CCl_4 was used as a scavenger[40] since the sample could be saturated with the liquid and saturation confirmed by the weight change. To determine its effect on the MLCT state, the emission intensity was measured in the presence and absence of CCl_4. Saturating a sample containing 1.9×10^{-6} mol of $Ru(bpy)_3^{2+}(ads)/g$ with degassed CCl_4 increases the emission intensity by 10–15%. Since there is no concurrent change in emission lifetime, the increase is attributed to a change in emission scattering due to a closer matching of the refractive index of CCl_4, 1.4601,[67] with that of PVG, 1.5.[68] CCl_4 does not quench the MLCT state, but it does affect the emission minimum and, in the presence of the analyzing beam, the net absorbance. Relative to the unsaturated sample, flash photolysis in the presence of degassed CCl_4 causes a 10% reduction in both the emission minimum and the net absorbance. Although CCl_4 always reduces the transient absorbance, the reduction varied from 5 to 27% for the different samples examined. The variation is attributed to differences in surface "wetting" since CCl_4 is insoluble in water and PVG has a polar surface with different amounts of chemisorbed water. Since Figure 6 is within experimental error of the spectrum of a solvated electron[66,69] and CCl_4 consistently reduces the transient absorbance, the primary photochemical step is attributed to a photoionization of $Ru(bpy)_3^{2+}(ads)$.

Discussion

The similarities and differences between PVG surfaces and those of other hydroxylated silicas have been described.[51-53] Both possess slightly acidic surface hydroxyls,[70] and as found with other hy-

droxylated silicas,[71-73] $Ru(bpy)_3^{2+}$ cation exchanges onto PVG without coadsorption of Cl^-. The absorbance of $Ru(bpy)_3^{2+}(ads)$ increases linearly as the moles adsorbed increases and impregnation via cation exchange is reproducible from sample to sample. Spectra of different locations on the same sample are also within experimental error and establish uniform distributions of the adsorbed complex on the surface.[44] Optical density vs. relative thickness indicates a nonuniform cross-sectional distribution in which the complex penetrates only 0.4 ± 0.1 mm into PVG. Since similar penetration depths are found with a variety of metal complexes which differ from $Ru(bpy)_3^{2+}$ in molecular size and mechanism of adsorption,[48,55,56,74] the depth indicated by grinding is taken as a measure of deviations from surface planarity rather than penetration into interior cavities. The linearity of optical density vs. optical path length (relative thickness), however, indicates that the concentration, i.e., the moles of $Ru(bpy)_3^{2+}$-(ads)/unit volume of PVG, is constant, which suggests that the complex is uniformily distributed among sites within the impregnated regions.

Electronic spectra of $Ru(bpy)_3^{2+}$ incorporated into silica colloids[37] or intercalated[75] into hectorite, a magnesium silicate, differ from fluid solution spectra. Relative to the MLCT band intensity, that of the 300-nm $\pi-\pi^*$ transition occurs in a ratio of 6:1 in aqueous solution, but reduces to 2:1 in the silicate.[75] The change is attributed to distortions of the bpy ligand imposed by the adsorbent. In contrast, $Ru(bpy)_3^{2+}$ cation exchanges onto the outer surfaces of PVG and retains UV–visible and resonance Raman spectra within experimental error of the aqueous solution spectra.[56] Consequently, $Ru(bpy)_3^{2+}(ads)$ is not subject to similar molecular distortions, and, at least in the ground state, the adsorbed complex is equivalent to that in aqueous solution. This does not imply that the complex is less strongly adsorbed. Desorption is not spectrally detectable when an impregnated sample is placed in distilled water, but requires an exchangeable cation.

The emission maximum, 610 nm, is also similar to that in fluid solution spectra.[42] The emission intensity increases linearly with I_a, but declines when the loading exceeds $\geq 10^{-4}$ mol/g.[56] The decline is attributed to self-quenching since, assuming a 7.4-Å molecular radius and $130-m^2/g$ surface area, it occurs at essentially monolayer coverage within the impregnated region. Below monolayer coverage, the $Ru(bpy)_3^{2+}(ads)$ emission quantum yield is 0.12 ± 0.03[56] compared with 0.042 ± 0.002 in degassed aqueous solution.[76] The change in ϕ_{em} is not accompanied by a change of similar magnitude in lifetime; the luminescent lifetime of the adsorbed complex is 740 ± 20 ns as compared with 600 ± 20 ns in degassed aqueous solution.[3] Therefore, the increase in ϕ_{em} for the adsorbed complex is due principally to an increase in the radiative decay rate. Resonance Raman spectra suggest that the increase is most likely a consequence of an altered excited-state structure.

The equivalence of the resonance Raman vibrational frequencies of $Ru(bpy)_3^{2+}(ads)$ with those of the complex in aqueous solution established that the ground state of the adsorbed complex is equivalent to that in aqueous solution. However, the relative intensity of the $1492-cm^{-1}$ vibration of $Ru(bpy)_3^{2+}(ads)$ is reduced by ca. 50% compared with the relative intensities in the aqueous solution spectrum. Being the most intense band, the $1492-cm^{-1}$ vibration plays a significant role in distorting the ground-state structure to that of the excited state.[56] Its reduction in intensity implies that the MLCT state populated during 450-nm excitation of the adsorbed complex differs from that in aqueous solution. If the structural difference carries over, or is magnified in view of the Stoke's shift, to the emissive MLCT state, then the structural

(66) Matheson, M. S. *Adv. Chem. Ser.* **1965**, *No. 50*, 46.
(67) "Handbook of Chemistry and Physics", 64th ed., 1983, C-373.
(68) Elmer, T., Corning Glass Co., private communication, 1980.
(69) Dorfman, L. M. *Adv. Chem. Ser.* **1965**, *No. 50*, 36.
(70) Iler, R. K. "The Chemistry of Silica", Wiley-Interscience: New York, 1979; pp 622–714.

(71) Ahrland, S.; Crenthe, I.; Noren, B. *Acta Chem. Scand.* **1960**, *14*, 1059.
(72) Stanton, J. H.; Maatman, R. W. *J. Colloid Sci.* **1963**, *18*, 132; *J. Phys. Chem.* **1964**, *408*, 237.
(73) Wolf, F.; Heyer, W. *Z. Anorg. Allg. Chem.* **1974**, *408*, 237.
(74) Kennelly, T., Ph.D. Thesis, City University of New York, 1980.
(75) Krenske, D.; Abdo, S.; VanDamme, H.; Crutz, M.; Fripiat, J. J. *J. Phys. Chem.* **1980**, *84*, 2447; **1981**, *85*, 797.
(76) Van Houton, J.; Watts, R. J. *J. Am. Chem. Soc.* **1976**, *98*, 4853.

difference may account for the increased emissivity of the adsorbed complex.

The spectral properties of the photoproducts, the reaction stoichiometry, and the intensity dependence establish a biphotonic induced disproportionation, reaction 1. In the photoinduced disproportionation of $Ru(bpy)_3^{2+}$ in aqueous solution, a thermal back reaction limits the lifetime of $[Ru(bpy)_2(bpy^-)]^+$ to 2.0 ± 0.6 ms.[40] The lifetime of $[Ru(bpy)_2(bpy^-)]^+$(ads), $\geqslant 48$ h in vacuo,[39] suggests that disproportionation of the complex on PVG occurs without the complementary thermal back reaction:

$$Ru(bpy)_3^{3+}(ads) + [Ru(bpy)_2(bpy^-)]^+(ads) \rightarrow$$
$$2Ru(bpy)_3^{2+}(ads) \quad (2)$$
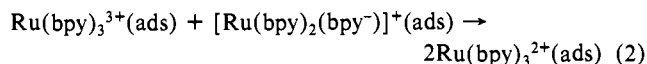
in spite of the latter's 2.5-eV driving force. The lack of reversibility cannot be attributed to either a change in the reaction products or, as occurs on cellophane, a competitive reduction of $Ru(bpy)_3^{3+}$(ads) by the support.[38]

Oxidation of PVG would most likely entail oxidation of chemisorbed water resulting in O_2 formation. Yet, GC analysis of the cell contents after exhaustive photolysis of a sample containing 1.2×10^{-5} mol of $Ru(bpy)_3^{2+}$(ads), 2.5×10^{-6} mol/g, indicates $\leqslant 10^{-7}$ mol of O_2. Optical and EPR spectra of $[Ru(bpy)_2(bpy^-)]^+$(ads) and the EPR spectrum of $Ru(bpy)_3^{3+}$(ads) are equivalent to those in 77 K glasses,[62,63] and remain unchanged for at least 2 h after photolysis. Adsorption does not significantly curtail thermal reactivity, since exposing a photolyzed PVG sample to O_2 oxidizes $[Ru(bpy)_2(bpy^-)]^+$(ads). The accompanying spectral changes indicate a $\geqslant 90\%$ regeneration of $Ru(bpy)_3^{2+}$(ads).

Nor are the data consistent with impurity quenching. EPR spectra give no indication of transition metal ions, although these are detectable in the ppm range in inorganic oxides.[77] Furthermore, product yield and stability are independent of whether calcining is carried out in an oxidizing, O_2, or reducing, H_2, atmosphere. Impurity quenching, which by some undefined means generates the observed redox products without an accompanying thermal back reaction, would occur with a 1:1 stoichiometry, and the photoproducts, would appear during the lifetime of the MLCT state, 740 ± 20 ns. Neither condition is met; the stoichiometry is 0.48 ± 0.05 and there is a 3–4 μs delay in the appearance of $[Ru(bpy)_2(bpy^-)]^+$(ads).

In developing a model for the disproportionation reaction and accounting for its lack of reversibility, the question of surface mobility on PVG is crucial. However, the current evidence regarding the mobility of $Ru(bpy)_3^{2+}$ ion-exchanged onto different supports at room temperature is mixed. Studies of the quenching of $*Ru(bpy)_3^{2+}$(ads) on PVG by various gases suggests that weakly adsorbed molecules migrate on the surface whereas the strongly adsorbed, ionically bound $Ru(bpy)_3^{2+}$(ads) does not.[44] In contrast, Thornton and Lawrence find that intensity and lifetime quenching of $*Ru(bpy)_3^{2+}$ by Cu^{2+} on a Sephadex-SP cation-exchange resin are within experimental error which suggests either long-range electron transfer or that one or both of the adsorbates are mobile.[78] Emission polarization measurements show that, at room temperature, 22 ± 1 °C, the emission of $Ru(bpy)_3^{2+}$(ads) exhibits a polarization ratio, P, of 0.12 ± 0.04,[56] which is within experimental error of the ratio found in low-temperature, 77 K, ethanol glasses.[79] Emission polarization implies that rotational motion of adsorbed complex is restricted. Since it is difficult to envision translational motion without concurrent rotational motion (we expect that translational mobility of $Ru(bpy)_3^{2+}$(ads) would occur by the complex tumbling across the PVG surface from site to site), we conclude that the translational motion of $Ru(bpy)_3^{2+}$(ads) is nonexistent and the complex remains fixed to a specific site. The linearity of $Ru(bpy)_3^{2+}$(ads) absorbance with relative thickness implies that half of the moles of $Ru(bpy)_3^{2+}$(ads), n, is uniformly distributed within a volume of PVG defined by geometric area of one side, A, and the penetration depth, d. The mean separation

between the adsorbates is, therefore, $(AdpS/Nn)^{1/2}$, where p and S are the density, 1.38 g/mL, and surface area, 130 m²/g, and N is Avogadro's number. The mean separations calculated for the various amounts of $Ru(bpy)_3^{2+}$(ads) are superimposed onto Figure 3.

The photoproducts are not luminescent, but the constant experimental difficulty of ensuring a correspondence between the region photolyzed and that analyzed suggests that macroscopic mobility is restricted. To establish the point, a 1-mm diameter region at the center of a 25 mm × 25 mm PVG sample containing 2.1×10^{-6} mol of $Ru(bpy)_3^{2}$(ads)/g was photolyzed, and the absorbance of $[Ru(bpy)_2(bpy^-)]^+$(ads) at 510 nm was monitored for 8 h after photolysis. Either diffusion of the reactant into or photoproduct out of the exposed region would cause a change in optical density. Within a experimental error of 4%, however, the optical density of the photolyzed region did not change which indicates that $\leqslant 8.4 \times 10^{-8}$ mol of $Ru(bpy)_3^{2+}$(ads) and $\leqslant 6.2 \times 10^{-9}$ mol of $[Ru(bpy)_2(bpy^-)]^+$(ads) diffused into or out of the exposed region. Since there is no spectral evidence of macroscopic mobility of the photoproducts and, like $Ru(bpy)_3^{2+}$(ads), $Ru(bpy)_3^{3+}$(ads) and $[Ru(bpy)_2(bpy^-)]^+$(ads) remain cationic throughout the reaction sequence, we assume that these complexes also remain ionically bound to specific sites. Therefore, the reaction system is a fixed array of immobile reactants which photolysis converts into a fixed array of immobile products.

The second-order dependence on excitation intensity indicates either a bimolecular reaction between two $*Ru(bpy)_3^{2+}$(ads) molecules or biphotonic excitation of an individual complex ion. Since the adsorbed complex is immobilized on the surface, the probability of a bimolecular reaction is a maximum at monolayer coverage, ca. 2×10^{-4} mol/g, when the ions are at a contact distance. Whether the decline in emission intensity at monolayer coverage involves annihilation[38] is not clear, but as indicated by Figure 3, ϕ_{Ru1} approaches zero as the loading approaches monolayer coverage. Consequently, a bimolecular reaction between $*Ru(bpy)_3^{2+}$(ads) molecules may compete with, but is not a precursor to, disproportionation on PVG. As found in aqueous solution,[40] biphotonic excitation of individual $Ru(bpy)_3^{2+}$(ads) initiates reaction 1. The rise time of the MLCT emission indicates that the lifetime of the state populated during 450-nm absorption is $\leqslant 10$ ns. Furthermore, the effect of O_2 on the flash photolysis signal, an 80% reduction in signal intensity, is within experimental error of O_2 quenching of the longer lived luminescent state. Since the emissive state absorbs at 450 nm ($\epsilon \sim 5 \times 10^3$ M⁻¹ cm⁻¹),[80] collectively these data suggest that biphotonic excitation is a sequential process in which the first photon generates the luminescent MLCT state which then absorbs the second photon.

Scavenging by CCl_4[40] and the similarity of Figure 6 to that of the solvated electron[66,69] indicate that the primary photoreaction is a biphotonic induced ionization. Assuming sequential excitation, the ionization energy, E, of $Ru(bpy)_3^{2+}$(ads) is $2.2 \leqslant E \leqslant 5.0 \pm 0.1$ eV. Energetically, the upper limit corresponds to direct 250-nm excitation and, in this sense, agrees with results in aqueous solution where excitation of $\leqslant 340$ nm enhances photoionization of the complex.[40] In aqueous solution, the photodetached electron either recombines with the oxidized complex or reduces a second $Ru(bpy)_3^{2+}$ leading to the observed disproportionation. With semiconductive supports such as SnO_2 and TiO_2, where the $Ru(bpy)^{3+/2+*}$ redox potential either matches or exceeds the potential of the conduction band,[31,32] the excited complex ejects an electron into the conduction band and the electron migrates to a reaction site. Kajiwara and co-workers have calculated a band gap of 6.9 eV for SiO_2 and place the conduction band potential (vs. NHE) at ca. -4.5 V.[32] Since PVG is an amorphous material with a hydrated surface,[51-53] most likely its respective values will be somewhat different from those of SiO_2. However, the absence of either lifetime or intensity quenching when the complex is adsorbed onto PVG and the excitation energies used in these experiments, $\leqslant 5$ eV, preclude on both kinetic and energetic
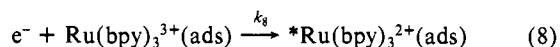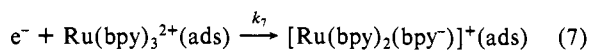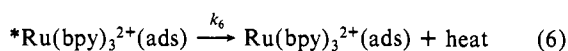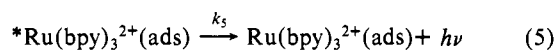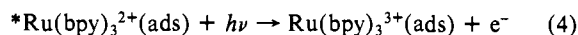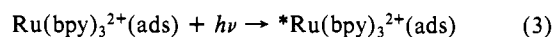
(77) Hentz, R. R.; Wickenden, D. K. *J. Phys. Chem.* **1969**, *73*, 817.
(78) Thornton, A. T.; Lawrence, G. S. *Chem. Commun.* **1978**, 408.
(79) Felix, F.; Forguson, J.; Gudel, H. U.; Ludi, A. *J. Am. Chem. Soc.* **1980**, *102*, 4096.

(80) Creutz, C.; Chou, M.; Netzel, T. L.; Okumura, M.; Sutin, N. *J. Am. Chem. Soc.* **1980**, *102*, 1309.

grounds mechanisms involving either adsorbate–adsorbent energy transfer or electron transfer to a PVG conduction band. Previous experiments have established photoionization of adsorbed molecules and ejection of electrons onto the PVG surface.[46,81–83] Consequently, we propose that biphotonic excitation ejects an electron onto the hydrated PVG surface. Analogy to disproportionation in aqueous solution[40] suggests the following reaction sequence:

$$Ru(bpy)_3{}^{2+}(ads) + h\nu \rightarrow {}^*Ru(bpy)_3{}^{2+}(ads) \qquad (3)$$

$$^*Ru(bpy)_3{}^{2+}(ads) + h\nu \rightarrow Ru(bpy)_3{}^{3+}(ads) + e^- \qquad (4)$$

$$^*Ru(bpy)_3{}^{2+}(ads) \xrightarrow{k_5} Ru(bpy)_3{}^{2+}(ads) + h\nu \qquad (5)$$

$$^*Ru(bpy)_3{}^{2+}(ads) \xrightarrow{k_6} Ru(bpy)_3{}^{2+}(ads) + heat \qquad (6)$$

$$e^- + Ru(bpy)_3{}^{2+}(ads) \xrightarrow{k_7} [Ru(bpy)_2(bpy^-)]^+(ads) \qquad (7)$$

$$e^- + Ru(bpy)_3{}^{3+}(ads) \xrightarrow{k_8} {}^*Ru(bpy)_3{}^{2+}(ads) \qquad (8)$$

Reactions 3 and 4 represent sequential excitation through the MLCT state and ionization. The lifetime, 740 ± 20 ns, and emission quantum yield, 0.12 ± 0.048[56] for *Ru(bpy)$_3{}^{2+}$(ads) yield 1.80 × 10^5 and 1.17 × 10^6 s^{-1} for k_5 and k_6, respectively.[84] Reaction 7 is reduction of another complex ion yielding [Ru-(bpy)$_2$(bpy$^-$)]$^+$(ads),[60–62] and reaction 8 is a chemiluminescent reduction of the oxidized complex. In aqueous solution, the latter occurs with a rate constant of ca. 6 × 10^{10} M^{-1} s^{-1} and populates the MLCT state in essentially unitary efficiency.[85] The reactions are equivalent to solution-phase reactions except that the reactants and products are fixed and the electron is the mobile intermediate.

The emission intensity at time t, $I(t)$, is directly proportional to the number of *Ru(bpy)$_3{}^{2+}$(ads), $n^*(t)$. However, reactions 3 through 8 cannot account for the emission minimum in Figure 5c since d$^2 n^*/$dt^2 is negative whenever d$n^*/$dt is zero. In other words, the rates of reactions 7 and 8 would be largest immediately after excitation when the number of electrons is largest. Since the Ru(bpy)$_3{}^{2+}$(ads) emission spectrum overlaps the absorption spectrum of e$^-$ (Figure 6), however, it is conceivable that an inner filter effect can achieve a local minimum. If so

$$I(t) = cn^*(t)[\exp(-\epsilon e^-(t))] \qquad (9)$$

where c is a proportionality constant and ϵ is the cross-sectional absorptivity of the electron on the glass. Therefore, attributing the sharp rise in $I(t)$ from 0.25 at $t = 0.83$ μs to 1.20 at $t = 1.25$ μs (Figure 5c) to an inner filter effect implies

$$1.20 = cn^*(1.25)[\exp(-\epsilon e^-(1.25))] \qquad (10)$$

and

$$0.25 = cn^*(0.83)[\exp(-\epsilon e^-(0.83))] \qquad (11)$$

Dividing (10) by (11) and realizing that $n^*(1.25) < n^*(0.83)$ yields

$$\exp(\epsilon \Delta e^-) \geq 4.8 \qquad (12)$$

where $\Delta e^- = e^-(0.83) - e^-(1.25)$. The decrease in e$^-$ occurs via reactions 7 and 8. Assuming that reaction 7 is negligible compared to reaction 8 (see below), since Ru(bpy)$_3{}^{3+}$ is a stronger oxidant than Ru(bpy)$_3{}^{2+}$ by 1.3 eV,[3] then $e^-(t) \simeq n^+(t)$, where $e^-(t)$ and $n^+(t)$ represent the number of e$^-$ and Ru(bpy)$_3{}^{3+}$(ads), respectively,

since $e^-(0) = n^+(0)$. Assuming equal amounts,

$$de^-/dt = -k_8(e^-)^2 \qquad (13)$$

whose solution is $e^-(0)/(1 + k_8 e^-(0)t)$. Substituting this into $\Delta e^- = e^-(0.83) - e^-(1.25)$ and rearranging yields

$$\Delta e^- = 2e^-(0)[5e^-(0)k_8/(6 + 5e^-(0)k_8)(4 + 5e^-(0)k_8)] \qquad (14)$$

Equation 14 achieves a maximum when $5e^-(0)k_8 = (24)^{1/2}$ with a maximum value of $1/(10 + 2(24)^{1/2})$. Therefore, ϵe^- is $\leq e^-(0)/9.9$, where $e^-(0)$ is the initial number of electrons. If the efficiency of photoionization is taken as 0.50, a rather generous estimate in view of the small values of ϕ_{Rul}, then excitation of 1.7 × 10^{-7} mol of Ru(bpy)$_3{}^{2+}$(ads) (the number of moles exposed to the laser pulse in a sample containing 2.0 × 10^6 mol/g) yields $e^-(0) = 8.5 \times 10^{-8}$ mol and $\Delta e^- \leq 8.6 \times 10^{-9}$ mol. Substituting $e^-(0)$ into (12) yields $\epsilon \geq 1.8 \times 10^8$ cm^2/mol. Considering that PVG has a hydrated surface and the cross-sectional absorptivity of e$^-$ in various protic solvents varies by $\leq 15\%$,[68] the calculated value of ϵ is unacceptably large when compared with the value of ϵ measured in water, 1.5×10^7 cm^2/mol.[66] This does not imply that absorption of the emission cannot occur. In fact, if ϵ is set equal to zero, the algorithm fails to fit the data in the 0.83 to 4 μs time span. The point here is that during the reaction sequence in which the number of electrons is declining with increasing time, the product ϵe^- is insufficient to attribute the minimum and the following pronounced rise in emission intensity in Figure 5c to solely an inner filter effect due to absorption of the *Ru-(bpy)$_3{}^{2+}$(ads) emission by e$^-$.

To account for this increase in emission intensity and the delay in [Ru(bpy)$_2$(bpy$^-$)]$^+$(ads) appearance, our calculations indicate that a significant number of photodetached electrons reside on the PVG surface for a finite period of time. We can only speculate as to the nature of the events during this time. It could represent the time required to thermally equilibrate or population of specific sites on the surface. These events are modeled by the reaction

$$e^- + S \xrightarrow{k_{15}} S^- \qquad (15)$$

S$^-$ does not represent F centers within the glass matrix as found in γ-irradiated PVG,[46,86,87] only that there exists on this surface a means to store, perhaps by population of prevalent Lewis acid sites,[52,88] this reactive intermediate. If the reactants are immobilized on the surface, however, then there must also exist a mechanism by which the electrons, if they populate surface storage sites, are reactivated for reactions 7 and 8 to occur. Since it would demand an unacceptably large ϵ, optical excitation is unlikely. On the other hand, the majority of the excitation energy, $\geq 85\%$, is dissipated as heat. Heat accumulates at a rate equal to the nonradiative rate, $k_5 = 1.17 \times 10^6$ s^{-1}, less the rate of heat flow into the bulk of the support. Particularly with poor thermal conductors such as PVG or SiO$_2$[89] and laser excitation, where the power density is high, thermal energy may play a significant role in the subsequent chemistry. We believe that the photodetached electrons populate surface sites and are thermally excited from these sites. The correlation between the 1/e time for nonradiative decay, 0.85 μs, and the time, 0.83 μs in Figure 5c, at which the emission intensity begins to increase due to reaction 7, alludes to its involvement here.

Designating Ru(bpy)$_3{}^{2+}$(ads), *Ru(bpy)$_3{}^{2+}$(ads), and Ru-(bpy)$_3{}^{3+}$(ads) as n, n*, and n$^+$, the differential equations corresponding to the events after excitation, reactions 5–8 and 15, are

$$d(n^*)/dt = -(k_5 + k_6)(n^*) + k_8(e^-)(n^+) \qquad (16)$$

$$d(n)/dt = (k_5 + k_6)(n^*) - k_7(e^-)(n) \qquad (17)$$

$$d(n^+)/dt = -k_8(e^-)(n^+) \qquad (18)$$

(81) Wong, P. K. *Photochem. Photobiol.* **1974**, *19*, 391.
(82) Kinell, P. O.; Edlund, O.; Lund, A.; Shimizu, A. *Adv. Chem. Ser.* **1968**, *No. 82*, 311.
(83) Yamada, Y.; Hasegawa, A.; Muira, M. *Bull. Chem. Soc. Jpn.* **1968**, *42*, 1836.
(84) Birk, J. B. "The Photophysics of Aromatic Molecules"; Wiley-Interscience: New York, 1970; p 89.
(85) Martin, J. E.; Hart, E. J.; Adamson, A. W.; Gafney, H. D.; Halpern, J. *J. Am. Chem. Soc.* **1972**, *94*, 9238.

(86) Weeks, R. A.; Nelson, C. M. *J. Am. Chem. Soc.* **1960**, *43*, 399.
(87) Muha, G. M. *J. Phys. Chem.* **1966**, *70*, 1390.
(88) Hair, M. L.; Chapman, I. D. *J. Am. Chem. Soc.* **1966**, *49*, 651.
(89) Blackwood, O. H.; Kelly, W. C.; Bell, R. M. "General Physics"; Wiley: New York, 1963; p 188.

$$d(e^-)/dt = -k_7(e^-)(n) - k_8(e^-)(n^+) - k_{15}(e^-)[1 - H_{0.83}(t)]^+ +$$
$$\delta(t - 0.88)S^-(t) \quad (19)$$

$$d(s^-)/dt = k_{15}(e^-)[1 - H_{0.83}(t)] - \delta(t - 0.83)S^-(t) \quad (20)$$

where $\delta(t)$ is the Dirac delta function, and $H_c(t)$ is the unit Heaviside function (0 for $t < c$ and 1 for $t \geq c$).[80] In writing the equation for reaction 15, two assumptions have been made. First, the number of surface storage sites is in excess, and, second, although this is unlikely and contributes to the error, the electrons are ejected at a specific time. The rate constants $k_5 + k_6$, k_7, k_8, and k_{15} plus the absorption constant ϵ are determined by an iterative algorithm. Measured or estimated values of these constants are used to solve the above equations via a high-order Runge–Kutta scheme.[90] This solution is then used to solve the associated variational equations[91] by the R–K scheme. The computed value of $I(t)$ is compared with the observed $I(t)$, and with the aid of the variational equations new values of the parameters are calculated. This process is repeated until convergence is obtained.

The algorithm was implemented twice: first, to match the observed $I(t)$ in the interval 0.5 to 4.0 μs and, second, in the interval 1.0 to 4.0 μs. The former case yields a reasonable fit swith a least-squares error of 0.68. Notice in Figure 5c, however, where the calculated values of $I(t)$ are superimposed on the observed values, that $\geq 84\%$ of the error occurs in the initial rapid decay. The recent experiments of Milosaviljevic and Thomas[38] and Kajiwara and co-workers[32] indicate rapid, nonexponential components in the decay of *Ru(bpy)$_3^{2+}$ adsorbed onto colloidal silica or SiO$_2$. Biphotonic excitation of the complex adsorbed onto PVG also reveals a rapid ($t \leq 50$ ns), nonexponential decay.[58] We incorporated some nonexponential decay processes into the reaction scheme, but when implemented on the computer, the corresponding algorithm either failed to converge, or the best fit of Figure 5c occurs with their rate constants equal to zero. We believe that nonexponential pathways play a role in the initial rapid decay, but their relation to the slower events examined in these experiments is not presently clear. In the latter case, i.e., in the 1.0- to 4.0-μs interval, however, the algorithm reproduces Figure 5c with a least-squares error of 0.011.

In matching $I(t)$ in the 1.0- to 4.0-μs interval, the algorithm yields $1.9 \pm 0.1 \times 10^6$ s^{-1} for $k_5 + k_6$ and 6.1×10^6 s^{-1} for k_{15}. A significantly larger estimate of $k_5 + k_6$ occurs when the algorithm attempts to match $I(t)$ in the 0.5- to 4.0-μs interval, but this reflects the algorithm's attempt to fit the initial rapid decay. Even in the shorter time interval, the value of $k_5 + k_6$ is still larger than that measured under low intensity excitation, $1.35 \pm 0.04 \times 10^6$ s^{-1}.[44] The calculated value of $k_5 + k_6$, however, is very sensitive in that slight changes, within the experimental error, in $I(t)$ cause large changes in their calculated value. This sensitivity is not present in fitting $I(t)$ in the 0.5- to 4.0-μs interval. Thus, further refinements in the calculated rate constants must await an understanding of the initial rapid decay and its relation to these events. The calculated values of k_7 and k_8, $2.2 \pm 0.1 \times 10^{12}$ and $2.2 \pm 0.1 \times 10^{13}$ cm^2/mol·s, respectively, differ by an order of magnitude. In contrast, the reactions between the hydrated electron and Ru(bpy)$_3^{2+}$ or Ru(bpy)$_3^{3+}$ in aqueous solution are diffusion limited and occur with essential identical rate constants of $7 \pm 1 \times 10^{10}$ M^{-1} s^{-1}.[59-61,85] Apparently, the reactions on this surface, where the electron initially populates a surface site, encounter energy barriers which magnify the difference in driving force (the driving force for reaction 8 is 0.5 eV larger than that for reaction 7) and discriminate between these reaction pathways.

The quantum yield of [Ru(bpy)$_2$(bpy$^-$)]$^+$(ads), ϕ_{Rul}, is

$$\phi_{Rul} = \phi_p f_{ej} k_7 / (k_7 + k_8) \quad (21)$$

where ϕ_p and f_{ej} represent the quantum efficiency of photoionization and the fraction of e$^-$ ejected from the surface storage sites.

Since the spectrum of the electron (Figure 6) is transient, f_{ej} is taken to be 1. Substituting the calculated rate constants and 1.1 $\times 10^{-4}$ for the maximum value ϕ_{Rul} yields 1.2×10^{-3} for ϕ_p. Since photoionization is a biphotonic event, ϕ_p reflects the efficiency of excitation of the MLCT state, and as such is a lower limit of the actual ionization efficiency. However, the value is similar to that reported by Meisel and co-workers for the yield of [Ru(bpy)$_2$(bpy$^-$)]$^+$, $1.5 \pm 0.2 \times 10^{-3}$, which represents a lower limit of the photoionization efficiency in aqueous solution.[40] The overall efficiency of reaction 1 appears to be limited principally by photoionization efficiency, and the competition between product formation, reaction 7, and recombination, reaction 8, the latter being the dominant process. Kajiwara and co-workers suggest that recombination limits, in part, the overall efficiency on TiO$_2$.[32]

Considering the involvement of surface sites as the initial electron acceptor, the dependence of ϕ_{Rul} on the moles adsorbed, Figure 3, might be interpreted to mean that only certain adsorption sites are active in promoting a net reaction. Excitation of the complex adsorbed onto a relatively small number of these sites, perhaps having an acceptor site nearby, leads to a net product formation, whereas excitation of molecules adsorbed onto other sites does not. Yet the latter sites, by eventually dominating the absorption, ultimately reduce ϕ_{Rul} to zero. Implicit in this proposal, however, is the assumption of preferential adsorption onto these reactive sites at low surface coverage. We would expect that this preferential adsorption, which implies a stronger adsorbate–adsorbent interaction, would be evident as changes in the adsorbate's spectral properties. VanDamme and Thomas and their co-workers, for example, describe significant changes in the absorption and emission spectra when Ru(bpy)$_3^{2+}$ is adsorbed into hectorite[75] or colloidal silica.[37] In our experiments, the absorption, emission, and resonance Raman spectra of Ru(bpy)$_3^{2+}$(ads) at low surface coverage, 5×10^{-7} mol/g, are identical with spectra at high surface coverage, 8×10^{-6} mol/g, and both are essentially identical with those of the complex in aqueous solution. Thus, attributing Figure 3 to preferential adsorption onto active sites is discounted. Rather, adsorption is a random process and, consistent with the assumption made in modelling reaction 15, the electron acceptor sites appear to be in excess.

Wong has established that electrons migrate on this surface,[81] whereas the data gathered here indicate that the reactants and products are fixed. Thus, Figure 3 is interpreted in terms of the mean separation between the adsorbate ions. As the moles of complex adsorbed/gram increases, the mean separation between the adsorbed ions decreases and approaches a separation distance within the electron migration distance. Consequently, the probability of reaction 1 increases. The maximum yield occurs at 2 $\times 10^{-6}$ mol/g which corresponds to a mean electron migration distance of 50 ± 10 Å. The value is in excellent agreement with Wong's determination of a 49-Å[81] and Wong and Allen's estimate of a 30-Å[46] mean electron migration distance in PVG. Furthermore, although electrical conductivity of amorphous solids depends on the method of preparation, surface structure, and surface impurities, the value is similar to the 34-Å electron migration distance in SiO$_2$ reported by Berglund and Powell.[92] The separation between the disproportionation products, however, exceeds that for the thermally activated reverse reaction, reaction 2. Consequently, the latter is either severely restricted or prevented, and the net efficiency of the photochemical reaction, reaction 1, increases. Further increases in the amount of complex adsorbed/gram decreases the mean separation between the disproportionation products and increases the probability of the reverse reaction. Consequently, the net efficiency declines. Figure 5 indicates that the reverse reaction dominates, i.e., ϕ_{Rul} approaches zero, when the loading exceeds 2×10^{-5} mol/g. This corresponds to a mean Ru–Ru separation of 20 ± 10 Å. Taking 7.4 Å, the diameter of Ru(bpy)$_3^{2+}$(ads), as the diameters of Ru(bpy)$_3^{3+}$(ads) and [Ru(bpy)$_2$(bpy$^-$)]$^+$(ads), the Ru–Ru separation indicates that the distance between the coordination shells must be ≤ 13 Å for the thermal back reaction to occur on PVG. Considering the larger

(90) Braun, M. "Differential Equations and Their Applications"; Springer-Verlag: New York, 1983; pp 111, 236.

(91) Coddington, E.; Levison, N. "Theory of Ordinary Differential Equations"; McGraw-Hill: New York, 1955; p 322.

(92) Berglund, C. N.; Powell, R. J. *J. Appl. Phys.* 1971, *42*, 573.

driving force for reaction 2, this result is in reasonable agreement with the findings of Guarr and McLendon which indicate that the thermal reactions between $Ru(bpy)_3^{3+}$ and homologues of methyl viologen, having driving forces of 0.1 to 0.6 V, require a mean separation between the reactants ranging from a contact distance to 10 Å in glycerol at 0 °C.[93]

Conclusion

These data indicate that disproportionation on PVG occurs via a reaction sequence very similar to that which occurs in aqueous solution.[40] Biphotonic excitation photoionizes the complex and the photodetached electron reduces a second $Ru(bpy)_3^{2+}$ ion. In aqueous solution, product lifetime is limited by the thermal back reaction which occurs because the products are free to diffuse about the reaction medium. On this support, however, the reactants are fixed, whereas the photodetached electron, after thermal excitation from initially populated surface sites, is a mobile intermediate. Consequently, disproportionation only occurs when the mean separation between the reacting adsorbate ions is within the electron migration distance. On the other hand, the electron migration distance, which these and other experiments indicate is on the order of 50 Å[46,81,92] exceeds the mean separation, ≤13 Å, necessary for the thermal back reaction, and the reaction

products are stable. Increasing the amount adsorbed increases the probability of the thermal back reaction by decreasing the mean product separation, and the quantum efficiency of the reaction declines.

This apparent "photochemical diode" effect[32] appears to arise from two factors on this support. First is the availability of electron acceptors sites on the surface. These are thought to be shallow energy wells from which the electron can be thermally activated but, nevertheless, present an energy barrier, albeit slight, which prevents immediate recombination. Energetically, they perform a function similar to band bending which promotes charge separation on the more conventional metal oxide semiconductors.[94] Second is that the electron migration distance exceeds that necessary for the thermal back reaction.

(93) Guarr, T.; McLendon, C., Abstracts, 182nd National Meeting of the American Chemical Society, New York, 1981: INORG 20.

(94) Novak, A. J., "Photochemical Conversion and Storage of Solar Energy"; Connolly, J. S., Ed.; Academic Press: New York, 1981; p 271.

CO Activation by Biscyclopentadienyl Complexes of Group 4 Metals and Actinides: η^2-Acyl Complexes[⊥]

Kazuyuki Tatsumi,[*†] **Akira Nakamura,**[†] **Peter Hofmann,**[*‡] **Peter Stauffert,**[‡] **and Roald Hoffmann**[*§]

Contribution from the Department of Macromolecular Science, Faculty of Science, Osaka University, Toyonaka, Osaka 560, Japan, Anorganisch-chemisches Institut der Technischen Universität München, D-8046 Garching, Federal Republic of Germany, and Department of Chemistry, Cornell University, Ithaca, New York 14853. Received October 9, 1984

Abstract: The electronic and geometrical structure and reactivity of η^2-acyl complexes of group 4 transition metals and of actinides are the subject of this paper. The directionality of the LUMO of d^0 Cp_2MI_2 systems favors a lateral or outside approach of a CO over a central one. Next the electronic structures of the η^2 acyls themselves are analyzed, and overlap reasons given for the preference for η^2 coordination in the Ti, Zr, and actinide complexes that are the main subject of this study, in contrast to the η^1 coordination in 18-electron Mn acyls. Our potential energy surfaces and qualitative analysis point to a preference for the O-inside η^2-acyl conformer for Ti and Zr, and approximately equal energies for O-inside and O-outside conformers for U and Th. We also find an unexpected η^1 minimum in the O-outside surfaces, with an orbital symmetry imposed barrier to slipping to the η^2 minimum. This suggests a pathway for the interconversion of the O-outside and O-inside η^2 isomers through an as yet unobserved η^1 structure. Separate oxycarbene isomers are also located, but these are at high energy. We believe the electrophilic reactivity of the η^2 acyls does not depend on reaching the oxycarbene isomers, but may be traced to a low-lying carbenium-ion-like acceptor orbital in the undistorted η^2-acyl structure.

Introduction

A particularly fascinating aspect of the activation of carbon monoxide by transition metal compounds is the carbonylation chemistry of biscyclopentadienyl dialkyls (diaryls), haloalkyls, and related derivatives of group 4 d metals[1] and of actinides,[2,3] Cp_2MR_2 and Cp_2MRX. CO insertion processes into the M–R bonds of these complexes are extremely facile and while not catalytic have

served as models for the CO activation and reductive CO coupling steps of some potentially industrially important catalytic processes.[4]

(1) (a) Fachinetti, G.; Floriani, C.; Marchetti, F.; Merlino, S. *J. Chem. Soc., Chem. Commun.* **1976**, 522–523. (b) Fachinetti, G.; Fochi, G.; Floriani, C. *J. Chem. Soc., Dalton Trans.* **1977**, 1946–1950. (c) Manriquez, J. M.; McAlister, D. R.; Sanner, R. D.; Bercaw, J. E. *J. Am. Chem. Soc.* **1976**, *98*, 6733–6735; **1978**, *100*, 2716–2724. (d) Wolczanski, P. T.; Bercaw, J. E. *Acc. Chem. Res.* **1980**, *13*, 121–127. (e) Erker, G. *Ibid.* **1984**, *17*, 103–109, and references therein. (f) Calderazzo, F. *Angew. Chem.* **1977**, *89*, 305–317. (g) Marsella, J. A.; Moloy, K. G.; Caulton, K. G. *J. Organomet. Chem.* **1980**, *201*, 389–398. (h) Baldwin, J. C.; Keder, N. L.; Strouse, C. E.; Kaska, W. C. *Z. Naturforsch.* **1980**, *356*, 1289–1297. (i) Jeffery, J.; Lappert, M. F.; Luong-Thi, M. T.; Webb, M. *J. Chem. Soc., Dalton Trans.* **1981**, 1593–1605. (j) Bristow, G. S.; Hitchcock, P. B.; Lappert, M. F. *J. Chem. Soc., Chem. Commun.* **1982**, 462–464. (k) Klei, E.; Teuben, J. H. *J. Organomet. Chem.* **1981**, *222*, 79–88. (l) For some related isocyanide chemistry, see: Wolczanski, P. T.; Bercaw, J. E. *J. Am. Chem. Soc.* **1979**, *101*, 6450–6452.